# The bizarre structure of the z = 3.4 radio galaxy B2 0902 + 343

C.L. Carilli

Leiden Observatory, Postbus 9513, NL-2300 RA Leiden, The Netherlands email: carilli@strw.leidenuniv.nl

Received 15 June / Accepted 22 September 1994

**Abstract.** We present high resolution (0.15'') radio continuum images of total and polarized intensity at 1.65 GHz of the z=3.4 radio galaxy B2 0902 + 343. These images were made by combining data from the VLA and MERLIN. Also presented is a re-analysis of the images of this source made with the VLA at higher frequencies (Carilli et al. 1994). The new high resolution low frequency image reveals a long 'plume' of emission extending well beyond the northern hot spot regions. This plume has an extremely steep spectrum (index  $\leq -3.3$ ), possibly indicating significant inverse Compton losses off the microwave background, as predicted for sources at very high redshift. High resolution spectral index images confirm that the southern-most knot in the jet has a flat spectrum (index  $= -0.03\pm0.02$  between 1.65 GHz and 8.3 GHz), suggesting it as the active nucleus of the radio galaxy.

The multifrequency polarized intensity images of B2 0902 + 343 verify the large rotation measures, and gradients in rotation measure, across the northern hot spot regions, indicative of a dense, magnetized local environment, comparable to what has been observed for lower redshift radio sources at the centers of cooling flow clusters. The high resolution 1.65 GHz image confirms the ring morphology of the southern-most component of the source, as previously seen at 8.3 GHz.

A detailed comparison between the radio and optical images of B2 0902 + 343 (from Eisenhardt & Dickinson 1992) is presented, showing how the flat spectrum radio core source is situated in a 'valley' between two optical peaks, and how the radio jet coincides closely with a 'trough' between the eastern and western parts of the optical galaxy.

We conclude that most of the peculiarities of the B2 0902 + 343 radio galaxy can be explained by assuming that the source is oriented at a substantial angle with respect to the sky plane, perhaps between  $45^{\circ}$  and  $60^{\circ}$ , with the northern regions of the source approaching. A requirement of this idea is that the central region of the galaxy be obscured by a substantial amount of dust.

**Key words:** galaxies: structures; B2 0902 + 343 – ratio continuum: galaxies

Send offprint requests to: C.L. Carilli

#### 1. Introduction

The first z > 3 radio galaxy to appear in the literature was that associated with the radio source B2 0902 + 343 at z = 3.40(Lilly 1988), and B2 0902 + 343 remains one of the more unique, and puzzling, of high redshift galaxies. The unique aspect of B2 0902 + 343 is its very flat optical broad band spectral energy distribution (SED), after correction for line contamination (Eisenhardt & Dickinson 1992; Eales et al. 1993). The flat SED of B2 0902 + 343, coupled with its low rest frame optical magnitude (relative to other high redshift radio galaxies), has led to the suggestion that B2 0902 + 343 is a prime candidate for a 'protogalaxy', undergoing its first major burst of star formation (Eales & Rawlings 1993; Eales et al. 1993; Eisenhardt & Dickinson 1992). The puzzling aspect of B2 0902 + 343 is that, unlike many high redshift radio galaxies, it does not follow the radio-optical 'alignment effect' (see McCarthy 1993 for a review). Indeed, the relative radio-optical morphology of B2 0902 + 343 is extremely bizarre, with the radio jet situated in a 'valley' between the twin-peaks seen in images of both broad band (R) continuum, and narrow band (Ly  $\alpha$ ) line, emission (Eisenhardt & Dickinson 1992). At z = 3.40,  $1'' = 3.5 h^{-1}$  kpc, where  $h = H_o/100 \,\mathrm{km} \,\mathrm{s}^{-1} \,\mathrm{M} \,\mathrm{pc}^{-1}$  and assuming  $q_o = 1/2$ .

The radio continuum properties of B2 0902 + 343 are also unusual. The radio source is fairly small (in projection) with a full extent of about 5''. The source shows a bright, 'knotty' jet of about 1.5'' extent, with a sharp bend of almost  $90^{\circ}$  at its northern end (Carilli et al. 1994; van Breugel & McCarthy 1989). The southern half of the source is comprised of two distinct components separated by about 1'' and situated about 3'' south of the jet. The position angle defined by the line connecting the two southern components is perpendicular to that of the source as a whole. The fainter of the two southern components forms a neat 'ring' of 0.4'' diameter when imaged at high spatial resolution. Another interesting result from the multifrequency polarized intensity images is the large rotation measures (>  $1000 \, \text{rad m}^{-2}$ ), and gradients in rotation measure, seen across the northern hot spot regions of B2 0902 + 343.

We have begun an extensive program of sensitive, high spatial resolution, multifrequency radio continuum imaging of high redshift radio galaxies to study the properties of the sources in

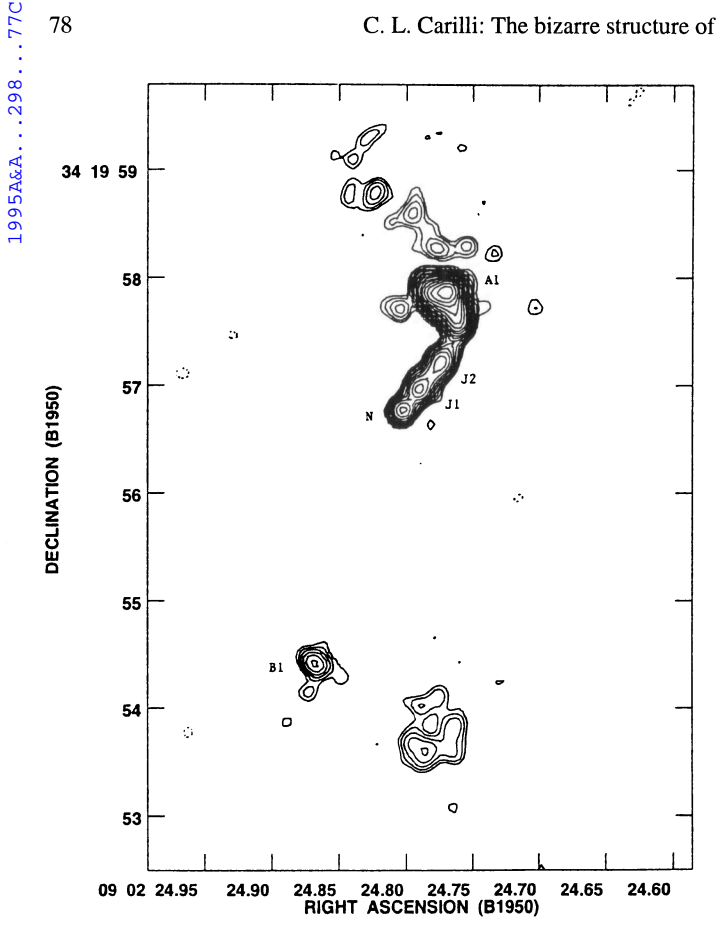


Fig. 1a. An image of total intensity from B2 0902 + 343 at 1.65 GHz with a resolution of 0.15'' (FWHM). The contour scheme is a geometric progression in  $2^{1/2}$ , which implies a factor 2 change in surface brightness every two contours (negative contours are dotted). The first level is 0.36 mJy/beam. The off-source RMS on this image is 0.12 mJy/beam

total and polarized intensity. Such observations are critical to the interpretation of the radio structures, and for comparison with high resolution optical images, and they provide unique information on the source environments. These studies include detailed observations of individual sources (Carilli et al. 1994), and a survey of a large number of z > 2 sources (Carilli et al. in prep). This paper presents images of total and polarized intensity of B2 0902 + 343 at 1.65 GHz with 0.15" resolution made from combined MERLIN+VLA data. Also presented is a reanalysis of the high frequency VLA observations of B2 0902 + 343. These data, combined with previous optical imaging, are used to develop a working model for the bizarre structures in the high redshift radio galaxy B2 0902 + 343.

## 2. Observations

A 12 hour dual polarization synthesis observation of B2 0902 + 343 at 1.65 GHz was made with the Multi-Element Radio Linked Interferometer (MERLIN) operated by the Nuffield Radio Astronomy Laboratory on January 1, 1994. The array consists of 8 elements with a maximum projected baseline length of 216 km and a minimum projected baseline length of 3.6 km (data from the very short MK2 to Lovell baseline were not used

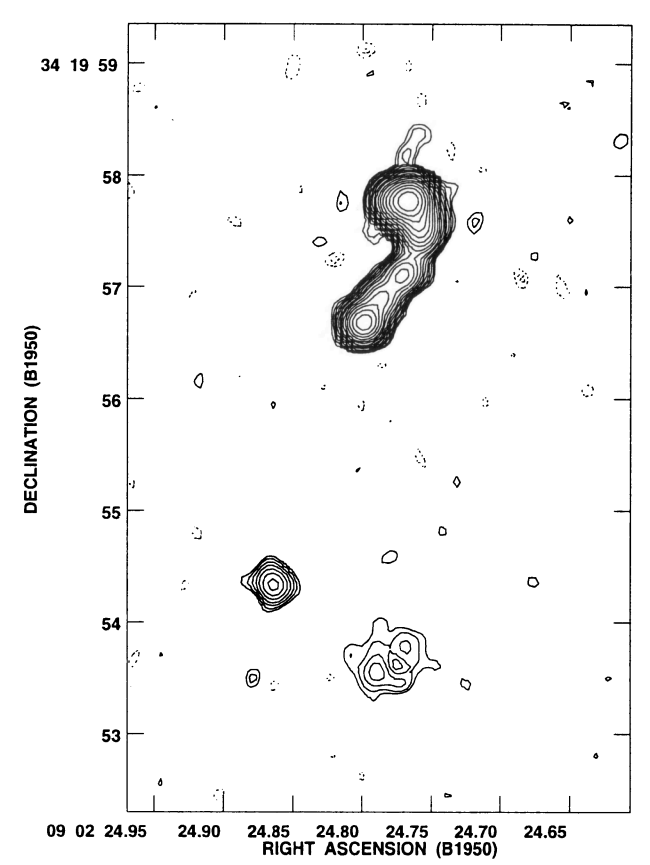


Fig. 1b. An image of B2 0902 + 343 at 8.3 GHz with a resolution of 0.21". The contour scheme is the same as Fig. 1a, but now the first level is 75 $\mu$ Jy/beam. The off-source RMS on this image is 25  $\mu$ Jy/beam

in this experiment). The MERLIN data were calibrated, edited, and self-calibrated by T. Muxlow using standard routines at NRAL.

A potential difficulty with the MERLIN-only data is the lack of short spacings in the Fourier-domain. Missing short spacings could lead to missing large-scale structure in the image plane, effectively putting the radio source in a 'hole' in the image plane. The shortest spacing used from the MERLIN data corresponds to a fringe which is sensitive to structures on scales of about 10". Hence, any diffuse structure on this scale associated with B20902 + 343 will not be properly imaged with the MERLIN only data. In order to fill-in these missing spacings, we added the short spacing (projected baselines < 5.4 km) VLA data at 1.65 GHz to the MERLIN data. Before the data were combined checks were made for relative astrometry and amplitude calibration. The relative VLA-MERLIN amplitude calibration was checked by looking at the visibility amplitudes on comparable projected baselines ('crossing points' in the uvplane). Agreement in amplitude was found to within 5%. The relative MERLIN-VLA astrometry was checked by comparing the position of the radio core of B2 0902 + 343 seen at 8 GHz with the VLA with that seen at 1.65 GHz with MERLIN at matched resolutions. The core position was found to agree to 0.1" between telescopes. A second check was made using the

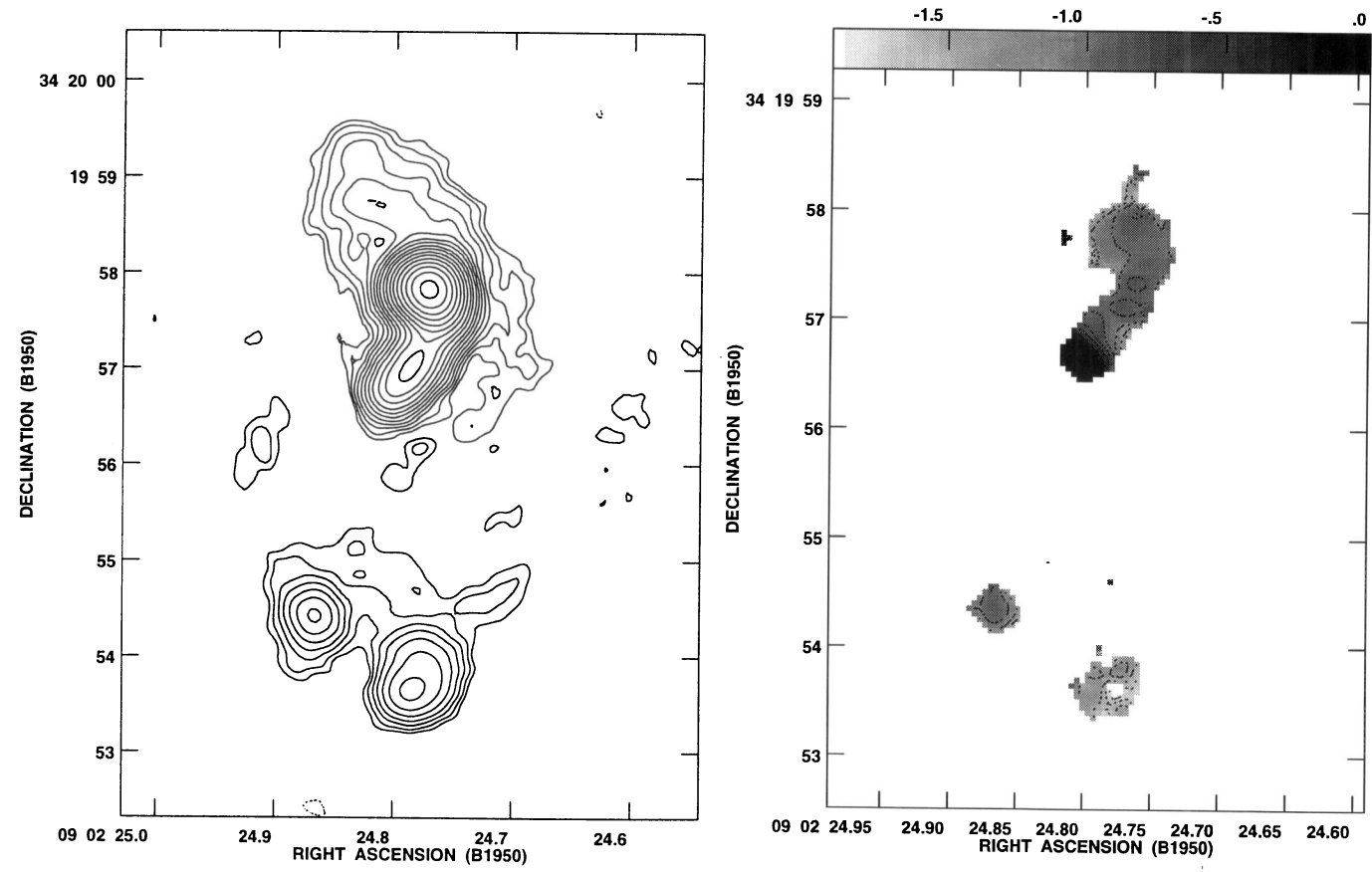


Fig. 1c. An image of B2 0902 + 343 at 1.65 GHz with a resolution of 0.4''. The contour scheme is the same as Fig. 1a, but now the first level is 0.55 mJy/beam

**Fig. 2a.** The greyscale and the contours are of the spectral index distribution of B2 0902 + 343 between 8.3 GHz and 1.65 GHz at 0.21" resolution. The contour levels are: -1.8, -1.6, -1.4, -1.2, -1.0, -0.8, -0.6, -0.4, -0.2, 0.0. The greyscale ranges from -1.9 (white) to 0.0 (black)

brightest hot spot (the A hot spot in the northern lobe), with a similar agreement between telescopes.

The VLA observations are described in detail in Carilli et al. (1994). In this paper we employ the data in the 5 GHz and 8 GHz bands of the VLA. These data were re-analyzed for the purposes of this paper in two ways. First, in each frequency band we observed at two frequencies separated by 450 MHz. The individual bands were analyzed independently in Carilli et al. (1994). In this paper the images of the Stokes parameters, I, Q, and U, from the two IF's in each band were combined to improve signal-to-noise. The median frequency is assumed in the analysis (4.7 GHz and 8.3 GHz). And second, the 1.65 GHz MERLIN image has revealed structure to the north of hot spot A. While this structure was suggested in the VLA higher frequency images, in our previous analysis the choice was made in the selfcalibration procedure to omit this structure, based on the false conclusion that the structure was an imaging artifact. The data has been re-analyzed with this new structure included in the self-calibration process.

## 3. Results and analysis

#### 3.1. Total intensity

A contour image of total intensity made from the MER-LIN+VLA data on B2 0902 + 343 at 1.65 GHz is shown in Fig. 1a. This image has been made using uniform weighting of the visibilities, and using a Gaussian taper of 1  $M\lambda$  (the taper distance corresponds to the 30% point of the Gaussian and  $\lambda$  is the observing wavelength). The spatial resolution, as defined by the FWHM of the Gaussian restoring CLEAN beam, is 0.15". For comparison, Fig. 1b shows the source at 8.3 GHz with a restoring beam of 0.21" FWHM. A number of features have been labeled, according to the nomenclature of Carilli et al. (1994).

The majority of the source structure is similar at both frequencies, with two notable exceptions. First, the southern-most component in the jet is considerably less prominent (relative to the the rest of the source structure) at low frequency than at high frequency. And second, the 1.65 GHz image reveals a long, spatially resolved 'plume' of emission extending well to the north of hot spot A. Fig. 1c shows an image at 1.65 GHz made using a Gaussian taper of 0.5  $M\lambda$ , resulting in a beam of

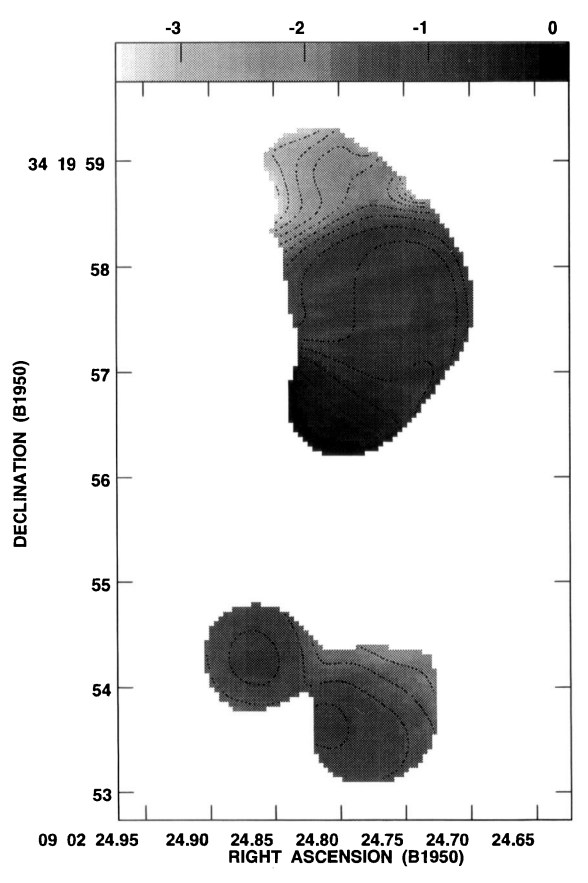
1995A&A.

Table 1. B2 0902 + 343 surface brightness and spectral indices

Component	Position <sup>a</sup>	F(1.65GHz) <sup>b</sup>	$lpha_{1.65}^{8.3~\mathrm{c}}$	$lpha_{8.3}^{15.0~ ext{d}}$
A1	09h02m24.77s, 34°19′57.85″	112	-0.86	-1.1
J1	$09^{h}02^{m}24.79^{s}, 34^{\circ}19'56.97''$	11.1	-0.80	-1.1
J2	$09^{h}02^{m}24.78^{s}, 34^{\circ}19'57.18''$	9.48	-0.74	-1.6
N	$09^{h}02^{m}24.80^{s}, 34^{\circ}19'56.78''$	9.57	-0.03	-0.5
B1	$09^{h}02^{m}24.77^{s}, 34^{\circ}19'54.42''$	2.81	-0.87	-

<sup>&</sup>lt;sup>a</sup>B1950

<sup>&</sup>lt;sup>d</sup>Spectral index between 8.3 GHzand 15.0 GHz at 0.21" resolution.



**Fig. 2b.** The greyscale and contours are of the spectral index distribution of B2 0902 + 343 between 4.7 GHz and 1.65 GHz at 0.4''. The contour levels are: -3.2, -2.9, -2.6, -2.3, -2.0, -1.7, -1.4, -1.1, -0.9, -0.7, -0.5, -0.3, -0.1, 0.0. The greyscale ranges from -3.5 (white) to 0.1 (black)

FWHM = 0.4''. At this resolution the plume is seen to extend about 2'' from hot spot A, to the northeast. The detection of this plume gives the radio source an overall 'S'-type symmetry about the center.

The hot spot B regions also show more diffuse structure at 1.65 GHz than at higher frequencies. In particular, the gap between the southern components and the core and jet to the north begins to fill-in with diffuse, steep spectrum emission.

## 3.2. Spectral Index

The spectral index distribution of B2 0902 + 343 between 1.65 GHz and 8.3 GHz at 0.21'' resolution is shown in Fig. 2a, where the spectral index,  $\alpha$ , is defined as: intensity  $\propto$  (frequency) $^{\alpha}$ . The values for peak surface brightness and spectral index between 8.3 GHz and 1.65 GHz for various source components are listed in Table 1. Also listed are spectral index values between 8.3 GHz and 15.0 GHz from Carilli et al. (1994) at this resolution.

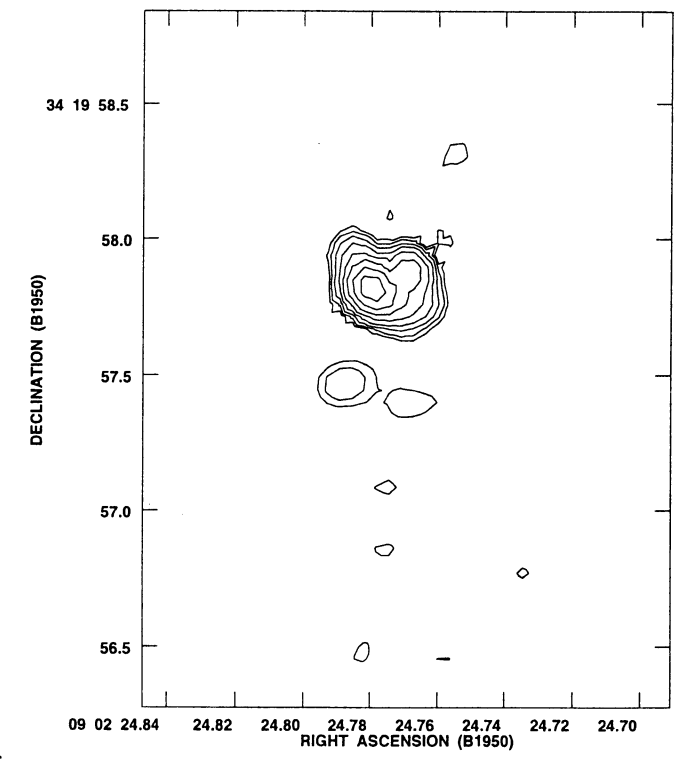


Fig. 3a. The linearly polarized intensity image of B2 0902  $\pm$  343 at 1.65 GHz at a resolution of 0.15". The contour scheme is the same as Fig. 1a, but now the first level is 0.5 mJy/beam. Note that only the northern region of the source is displayed, since this is the only region where polarized emission is detected

<sup>&</sup>lt;sup>b</sup>Surface Brightness in mJy/beam at 0.21" resolution (FWHM of Gaussian restoring beam) at 1.65 GHz.

<sup>&</sup>lt;sup>c</sup>Spectral index between 1.5 GHz and 8.3 GHz at 0.21" resolution.

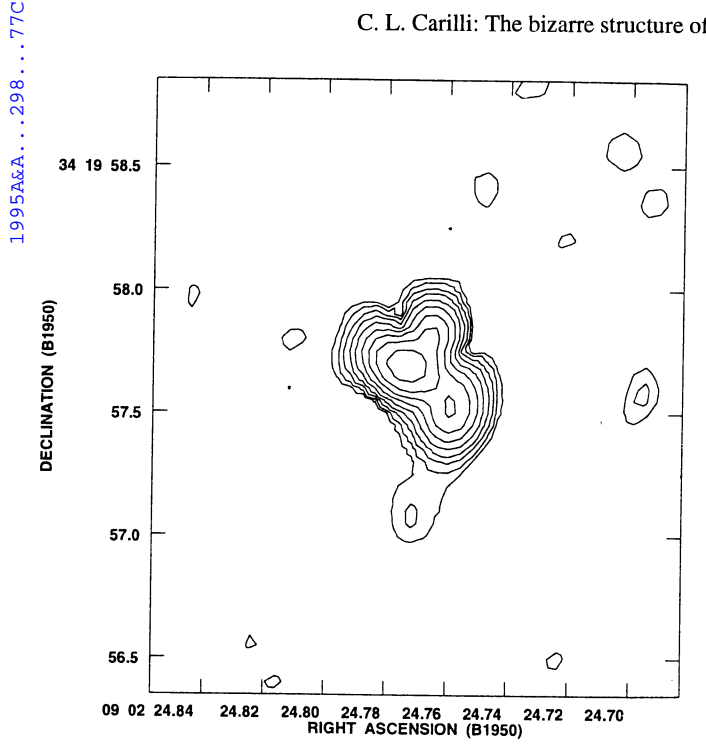


Fig. 3b. The linearly polarized intensity image of B2 0902 + 343 at 8.3 GHz at a resolution of 0.21". The contour scheme is the same as Fig. 1a, but now the first level is 0.1 mJy/beam

The southern-most component in the jet is seen to have a flat spectrum ( $\alpha_{1.65}^{8.3} = -0.03 \pm 0.02$ ). We assume, as in Carilli et al. (1994), that this component is the active nucleus of B2 0902 + 343. The spectral index distribution between 1.65 GHz and 4.7 GHz at 0.4" resolution is shown in Fig. 2b. The most remarkable aspect of this image is the plume to the north of hot spot A, which has an extremely steep spectrum, reaching a sensitivity limited minimum spectral index value of -3.3 (spectral index values were only calculated in regions where surface brightness was above four times the off-source RMS at each frequency). Note that, even with the plume, the full extent of the source is only about 7", which is below the 10" maximum size that can be properly imaged with a full synthesis observation with the VLA in A array at 4.7 GHz (Perley 1993).

#### 3.3. Polarized emission

The polarized intensity image of B20902 + 343 at 1.65 GHz with a resolution of 0.15" is shown in Fig. 3a, while Fig. 3b shows the polarized intensity at 8.3 GHz at 0.21" resolution. The only region with significant polarized emission at both frequencies is the region around hot spot A. The fractional polarization attains maximum values of about 12% at both 8.3 GHz and 1.65 GHz in this region. For comparison, the limit  $(1\sigma)$  to fractional polarization for hot spot B1 in the southern half of the source is  $\leq$  3% at both 1.65 GHz and 8.3 GHz. The 8.3 GHz image shows significant polarized flux from jet knot J2, with a fractional polarization of 5%. At 1.65 GHz the fractional polarization of J2 is < 0.9%.

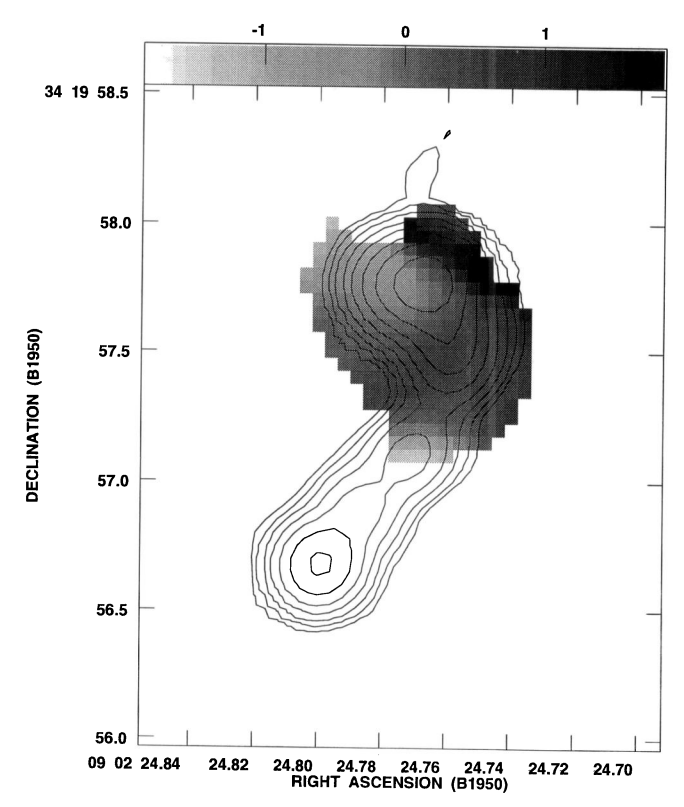
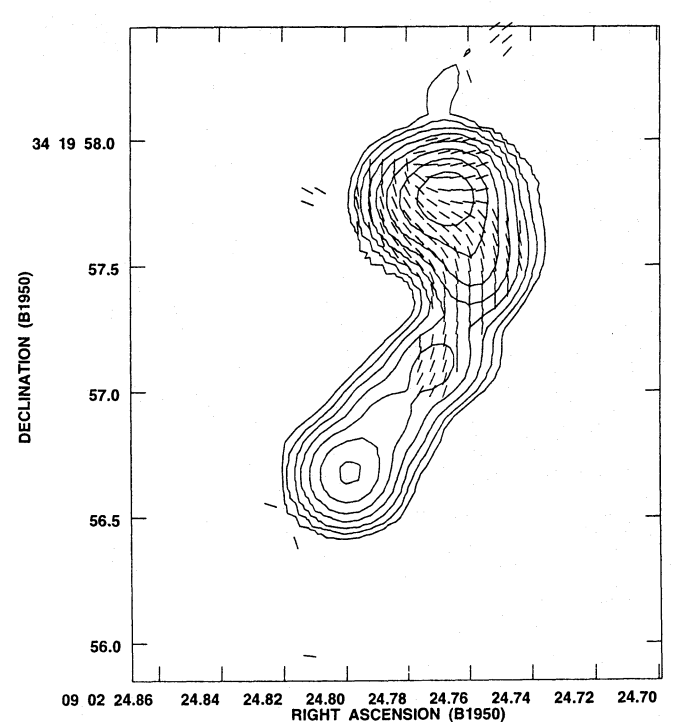


Fig. 3c. The contours are of total intensity from B2 0902 + 343 at  $8.3\,\mathrm{GHz}$  with a resolution of 0.4''. The greyscale is of Faraday rotation measure at 0.4" resolution. The greyscale range is -2000 rad  $\mathrm{m}^{-2}$  (white) to +2000 rad  $\mathrm{m}^{-2}$  (black), and the contour levels are: -0.18, -0.09, 0.09, 0.18, 0.36, 0.72, 1.44, 2.88, 5.76, 11.52, 23.04, 46.08 mJy/beam

The 1.65 GHz data provide an important check to the claim of large rotation measures, and rotation measure gradients, seen towards the A hot spot region of B20902 + 343 (Carilli et al. 1994). In Fig. 4 are shown plots of observed position angle versus wavelength<sup>2</sup> for two positions in B2 0902 + 343. Note that the analysis was necessarily done at 0.4" resolution, in order to include all three frequencies (8.3, 4.9, and 1.65 GHz). In all cases reasonable fits of observed position angle versus wavelength<sup>2</sup> are obtained, verifying the notion of large rotation measures, and gradients in rotation measure, towards B2 0902 + 343. The rotation measure distribution in the northern hot spot region (Fig. 3c), shows a gradual change of rotation measure from east to west, as well as a 'ridge' of large rotation measure running along northern edge of the radio source, perhaps indicative of compression of cluster gas by the expanding radio source (Carilli et al. 1988). As discussed in Carilli et al. (1994), the large rotation measures seen towards B2 0902 + 343 are indicative of a dense, magnetized local environment, comparable to what has been observed for radio sources at the centers of cooling flow clusters (Taylor et al. 1994).

We have transformed wavelengths into the rest frame of the source before calculating the rotation measure, implying a factor of  $(1 + z)^2$  larger rotation measures than if we used the observed wavelengths. We feel this transformation is reasonable



**Fig. 3d.** The contours are of total intensity from B2 0902 + 343 at 8.3 GHz with a resolution of 0.21". The line segments show the projected magnetic field direction, for regions with significant polarized flux

since rotation measure changes of  $\geq 50 \,\mathrm{rad}\,\mathrm{m}^{-2}$  over scales of less than an arc-second are hard to justify for a Galactic screen (Leahy 1987; Pedelty et al. 1989). The observed wavelength dependence of the fractional polarization of knot J2 is another indication of large rotation measures local to B2 0902 + 343 (Dreher et al. 1987).

The projected magnetic field morphology at 0.21" resolution is shown in Fig. 3d. The field projects parallel to the jet (to within 11°), and perpendicular to the edge of the lobe. The magnitude of the magnetic field can be estimated by assuming a minimum energy configuration for the fields and particles (Miley 1980). The question of the validity of assuming minimum conditions in radio sources remains open. However, support for such an assumption comes from the recent detection of synchrotron self Compton X-ray emission from the radio hot spots of Cygnus A, from which hot spot magnetic fields were derived independent of minimization assumptions. The results for Cygnus A were fields close to those derived from minimum energy assumptions (Harris et al. 1994). Making the same assumptions as in Carilli et al. (1991), we derive minimum energy fields in the hot spots of B2 0902 + 343 of 650  $\mu$ G, while those in the diffuse plume to the north of hot spot A are about 100  $\mu$ G. The implied minimum pressures are  $1 \cdot 10^{-8}$  dynes cm<sup>-2</sup> in the hot spots and  $3 \cdot 10^{-10}$  dynes cm<sup>-2</sup> in the lobes. For comparison, minimum energy fields in the lobes of Cygnus A are about  $50 \,\mu\text{G}$ , while those in the hot spots are about 300  $\mu\text{G}$  (Carilli et al. 1991; Harris et al. 1994).

#### 3.4. Radio-optical comparisons

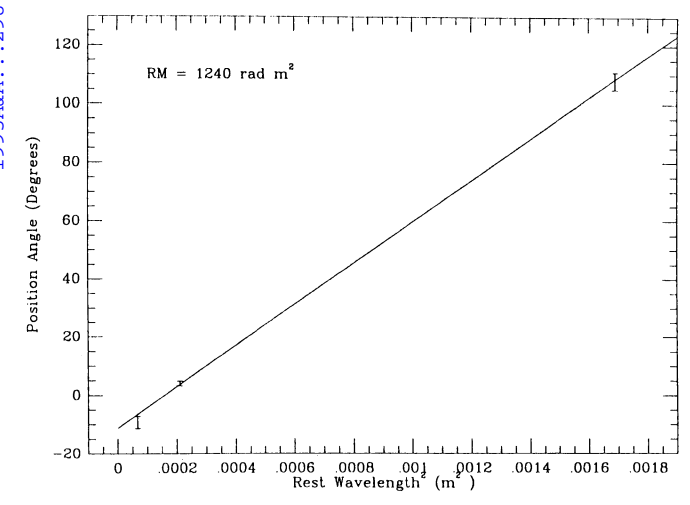
Broad and narrow band optical images of B2 0902 + 343 were presented in Eisenhardt & Dickinson (1992). In Fig. 5 we reproduce two of these images, along with images of the radio source at 1.65 GHz. Figure 5a shows the R band image of B2 0902 + 343. The R band redshifts to a relatively line free uv continuum band in the rest frame of B2 0902 + 343. Figure 5b shows the narrow band image centered on Ly $\alpha$  emission from B2 0902 + 343. Eisenhardt & Dickinson quote an optical seeing FWHM0.95". A cross marks the position of the flat spectrum radio core.

The relative radio-optical morphology of B2 0902 + 343 shows clearly the two remarkable aspects of the B2 0902 + 343 optical galaxy. First is the fact that both the continuum and line emission are asymmetrically distributed relative to the radio core source, with the majority of the emission coming from north of the radio core. Second is the east-west split of both the line and continuum emission, with the radio source being situated in between these two optical emission regions. Indeed, the northern jet and hot spot regions of the B2 0902 + 343 radio source fill almost exactly the trough between the optical peaks, and the radio core position corresponds to a 'valley' in both optical images.

A critical question in the above analysis is the accuracy of the astrometry. Again, we found the astrometry of the VLA to be consistent with that of MERLIN to within 0.1" (Sect. 2). Eisenhardt & Dickinson used seven stars in the field for astrometry, and quote standard deviation of 0.25". There is the additional question of the relative radio-optical reference frames. The recent compilation of Stone (1994) suggests a typical uncertainty between the two frames of  $\approx 0.2$ ". In order to have the radio core correspond to the nearest optical peak would require a shift of 1" between the radio and optical images. While possible, we feel such a large astrometric error to be unlikely, and we proceed under this assumption.

## 3.5. The ring

An interesting aspect of the southern lobe of B2 0902 + 343 is that one of the components forms a neat 'ring' of 0.4" diameter. The possibility of gravitational lensing for this component was considered in Carilli et al. (1994). A critical test of lensing is to observe how the morphology of this feature changes with wavelength. In Fig. 6 are shown high resolution images of the ring at both 8.3 GHz and 1.65 GHz. We see that the feature appears as a ring at both frequencies. There are some apparent differences in specific morphology around the ring between the two images. However, the signal-to-noise of the emission is insufficient to rule out a roughly constant spectral index around the ring of -1.4 (with substantial uncertainty, errors  $\pm 0.3$  in spectral index). No polarized emission is seen from the ring at either 1.65 GHz or 8.3 GHz. The implied fraction polarization limits in the brightest regions of the ring are 4% and 9%, respectively. Further consideration of the question of lensing for this ring component will be considered elsewhere (Hogg et al. in preparation).



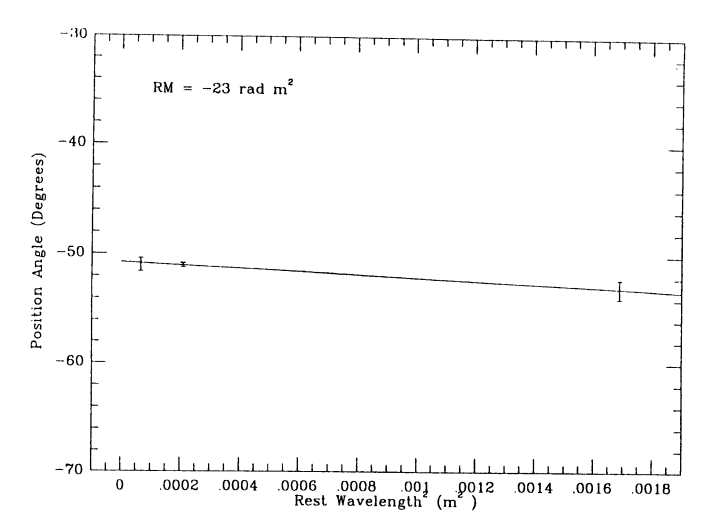


**Fig. 4.** The observed position angle as a function of (wavelength)<sup>2</sup> for the polarized emission from B2 0902 + 343. The observed wavelengths have been shifted to z = 3.4. All data are at 0.4'' resolution

## 4. Discussion

#### 4.1. Radio spectra

An interesting result in the spectral index distribution in B2 0902 + 343 is the extremely steep spectral index ( $\alpha \leq -3.3$ ) in the northern plume. This steep spectral index suggests an exponential cut-off in the emission spectrum, as would occur for a sharp cut-off in the electron energy spectrum. It is interesting to note that for well studied radio galaxies at lower redshift spectral steepening at high frequency tends to be more gradual than exponential. The steepest spectra observed tend to be no steeper than index  $\approx -2.2$ . This includes detailed observations of the lobes of high luminosity sources, such as Cygnus A (Carilli et al. 1991), and sensitive observations of diffuse, low luminosity sources in clusters, such as A2256 (Rottgering 1993). For the low redshift sources high frequency steepening more gradual than exponential may indicate the lack of pitch angle scattering in the electron distribution, or spatial variation in the magnetic field strength (Tribble 1993). However, for high redshift sources

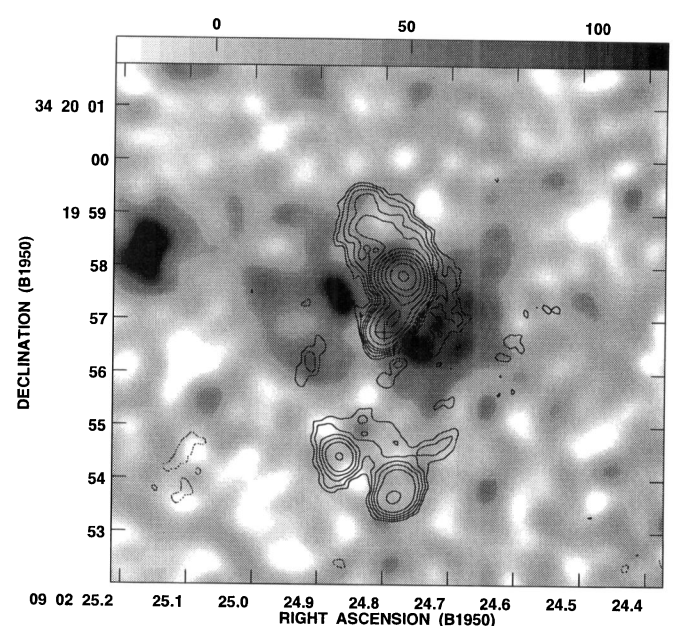
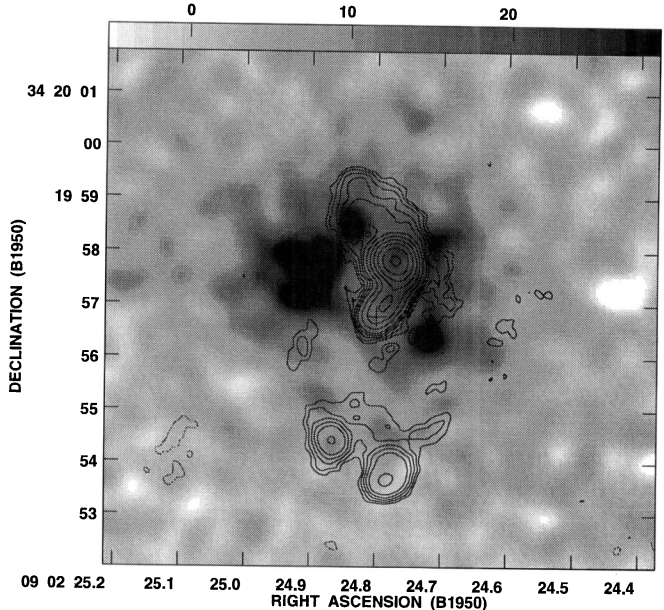


Fig. 5a. The greyscale is an optical R band image of B2 0902 + 343, reproduced from Eisenhardt and Dickinson (1992). The contours are the radio emission from B2 0902 + 343 at 1.65 GHz at 0.4" resolution. The contour levels are the same as Fig. 1c. A cross marks the position of the flat spectrum radio nucleus



**Fig. 5b.** The greyscale is an optical narrow band image of B2 0902 + 343 showing the Ly $\alpha$  emission, reproduced from Eisenhardt and Dickinson (1992). The contours are the radio emission from B2 0902 + 343 at 1.65 GHz at 0.4" resolution. The contour levels are the same as Fig. 1c

an exponential cut-off is unavoidable due to the rapidly increasing role of inverse Compton losses off the microwave background (MWBG) – an effect which is independent of the pitch angle distribution. The energy density of the MWBG evolves

as:  $U_{\rm BG} = 4.2\,10^{-13}(1+z)^4\,{\rm ergs\,cm^{-3}}$ . Hence, at z=3.4 the energy density in the MWBG is equivalent to that in a magnetic field of  $63\mu{\rm G}$ , and hence comparable to minimum energy fields in the lobes of high luminosity radio galaxies. As pointed out by Tribble (1993): 'the sharp spectral break should become more prominent for sources with lower field strength, or for sources at high redshift where inverse Compton losses are more important since  $U_{\rm BG}$  is much greater.'

The high resolution MERLIN images at 1.65 GHz allow for a more accurate determination of the core spectral index, and hence core fraction, for B2 0902 + 343. Using the core spectrum, and the spectrum of the total emission from B2 0902 + 343, implies a ratio of core flux density to total flux density of 2.4% at a rest frame frequency of 5 GHz. This value is intermediate between that of radio galaxies (typically  $\leq$  1%), and radio loud quasars (typically  $\geq$  a few %; Kapahi & Murphy 1990).

Constraining the flux density and spectrum of the nucleus also has implications on the interpretation of the associated HI 21cm absorption line system seen towards B2 0902 + 343 (Uson et al. 1991; Briggs et al. 1993). The spectral line observations do not spatially resolve the background source, leaving open two very different physical interpretations for the obscuring cloud. The first involves a large, low optical depth cloud ( $\tau \approx 0.01$ ), covering most, or all, of the radio source. In this case the neutral gas mass will be large,  $\geq$  few  $\times~10^{10}~h^{-2}\,M_{\odot}$  for a spin temperature of 10<sup>4</sup> (Uson et al. 1991). The alternative is a single, high optical depth cloud ( $\tau \geq 1$ ), covering a small fraction of the source - presumably the nucleus. In this case the cloud mass would be much smaller than above. We have found a flat spectrum nucleus in B2 0902 + 343, with a flux density of 10 mJy at 1.6 GHz. The maximum depth of the absorption line towards B2 0902 + 343 is  $11\pm2$  mJy. Hence, as long as the spectrum of the nucleus stays flat down to 323 MHz, it remains plausible that the absorption is due to a small, optically think cloud towards the nucleus. The final answer to this question will come with spectral line VLBI observations, to image the absorbing cloud against the background radio source.

The spectra for the knots in B2 0902 + 343 show significant curvature, steepening considerably from low to high frequency. The data are consistent with a model in which there is injection of a power law population of relativistic electrons with emission index between -0.5 and -0.7, and subsequent synchrotron and inverse Compton energy loses within the knots. Such a model has been successfully applied in the case of the hot spots in lower redshift radio galaxies (Carilli et al. 1991; Meisenheimer et al. 1989; Muxlow et al. 1988). The implied 'synchrotron break frequency' in hot spot A in B2 0902 + 343 is 11 GHz, which is similar to those found for the hot spots in Cygnus A and other lower redshift sources. The tentative conclusion is that there is no fundamental difference between relativistic particle acceleration and loss mechanisms in hot spots in high redshift sources than is seen for hot spots in lower redshift radio galaxies. This conclusion is admittedly weak, since we have only three observed frequencies for B2 0902 + 343 at high resolution. More observations at different, preferably lower, frequencies with similar spatial resolution are required

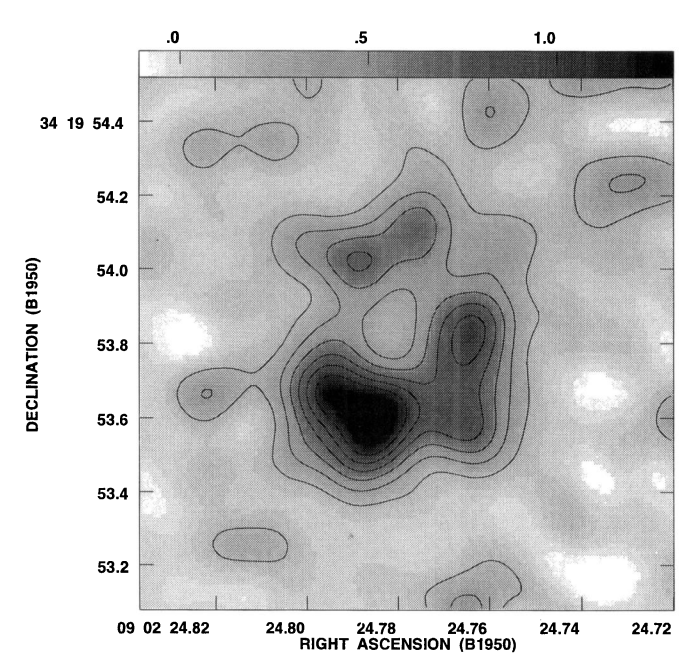


**Fig. 6a.** The greyscale and contours are of total intensity from the B2 component in the southern lobe (the 'ring') of B2 0902 + 343 at 1.65 GHz with a resolution of 0.15". The contour levels are: -0.18, 0.18, 0.36, 0.54, 0.72, 0.9, 1.08, 1.26, 1.44 mJy/beam. The greyscale ranges from -0.1 (white) to 1.3 (black) mJy/beam

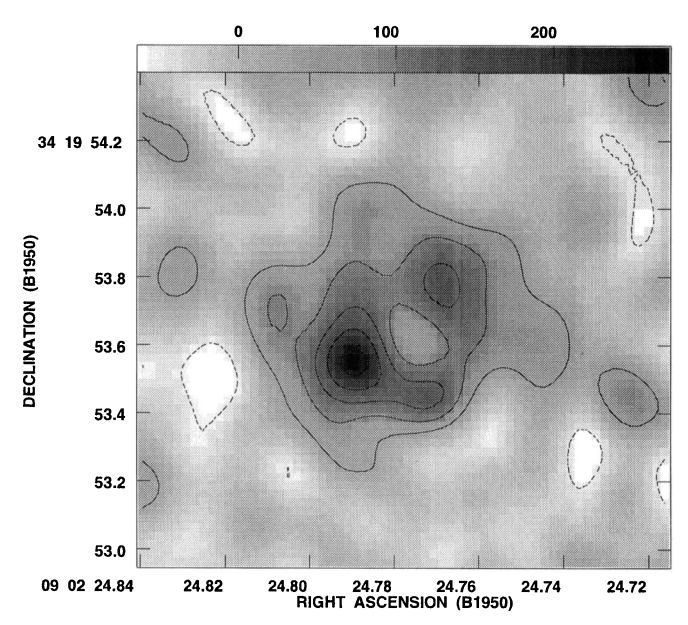


**Fig. 6b.** The greyscale and contours are of total intensity from the B2 component in the southern lobe (the 'ring') of B2 0902 + 343 at 8.3 GHz with a resolution of 0.21". The contour levels are: -0.05, 0.05, 0.1, 0.15, 0.2, 0.25 mJy/beam. The greyscale ranges from -0.06 (white) to 0.27 (black) mJy/beam

to better constrain the radio spectra of the knots in B2 0902 + 343.

4.2. B2 0902 + 343: a highly projected radio galaxy?

In total intensity the B2 0902 + 343 radio source shows a prominent jet, a very bent, 'S' shaped morphology, and a bright core, with a core-to-total flux density ratio intermediate between that typical of radio galaxies and that typical of quasars. In polarized intensity the only region with significant polarized flux at both 1.65 GHz and 8.3 GHz is the hot spot A region. All these features suggest a radio source which is at a significant angle with respect to the sky plane, with the northern regions approaching and the southern regions of the source receding (see also van Breugel & McCarthy 1989). In this model, hot spot A then 'pokes-out' of the denser line emitting regions in our direction, and hence avoids the expected Faraday depolarization (Pedelty et al. 1989; Baum & Heckman 1989; van Breugel et al. 1984).

A highly projected radio source in B2 0902 + 343 is also suggested by a number of other features. First is the steep spectrum plume revealed by the MERLIN observations. This plume extends to the north of hot spot A, i.e. to greater distances from the core than the hot spot itself. Such a morphology is inconsistent with the well accepted model for powerful radio galaxies in which the hot spot represents the 'working surface' of the jet, and the lobes represent the 'waste jet products' (Begelman et al. 1984). Projection could obviously alleviate this inconsistency. Second, if the rotation measure 'ridge' along the northern edge of the hot spot A region signifies enhanced Faraday rotation due to a bow shock preceding the radio source into the ambient medium, then the observed morphology requires significant projection in order to allow for the polarized emission from the radio source itself to back-light this screen (Carilli et al. 1988). And third, B2 0902 + 343 does not obey the radio-optical alignment effect, a common characteristic of radio galaxies at large redshifts (McCarthy et al. 1987; Chambers et al. 1987). Such an alignment could be hidden if the radio source, and its corresponding aligned optical emission, were at a significant angle with respect to the sky plane.

Given these observations, what angle,  $\theta$ , is implied for the B2 0902 + 343 radio source relative to the sky plane? In the context of theories for unification-by-orientation of radio loud quasars and radio galaxies (Antonucci 1993), the fact that the source morphology in B2 0902 + 343 is intermediate between that expected for a quasar and that expected for a radio galaxy suggests a source close to the transition angle between these objects, which, based on source statistics, is thought to be:  $\theta \sim 44^{\circ}$  (Barthel 1989).

Another limit to this angle can be found by assuming that hot spot A is situated on the near side of the denser line emitting regions. We have analyzed the azimuthally averaged radial profile of the line emitting gas centered on the radio nucleus. The profile shows a sharp drop in average surface brightness between 2" and 3", with a low surface brightness 'halo' extending to  $\geq 5$ ". The half-light radius is 2.5", and we use this as a characteristic radius for the denser line emitting gas (Fig. 5b). For the hot spot to extend beyond this radius implies a lower limit to the angle between the radio source and the sky of  $\theta > 60^{\circ}$ . We estimate that a similar value of  $\theta \geq 60^{\circ}$  would be adequate

to 'mask' the radio-optical alignment effect in B2 0902 + 343 by projection.

While none of the above arguments is compelling, the fact remains that assuming a highly projected radio source in B2 0902 + 343 solves many of the peculiarities for the source. One difficulty with this conclusion is that the required angle appears to be somewhat larger than the 'standard' quasar-radio galaxy transition angle. Hence, we would expect to see considerable quasar-like tendencies in the optical images and spectra of B2 0902 + 343, e.g. broad wings to the emission line profiles and a blue galaxy nucleus. Contrary to this expectation, the observed Ly $\alpha$  width in B2 0902 + 343 is typical of narrowline radio galaxies (Lilly 1988), and no optical point source is detected at the position of the radio core source. Perhaps this indicates an exceptional amount of obscuration by dust in B2 0902 + 343? Eisenhardt & Dickinson (1992) point out that substantial obscuration by a kpc-scale dust distribution could also explain the unusually high [O III]-to-Ly $\alpha$  ratio in B2 0902 + 343, and the spatial variation in the R-K color. It is interesting to note that a massive, kpc-scale dust distribution has recently been proposed for the z = 3.80 radio galaxy 4C 41.17 (Dunlop et al. 1994).

Still, while it is natural to assume that dust may obscure the center of the galaxy, the question remains as to why there is such a close spatial coincidence between the 'trough' in the optical images (both line and continuum), and the northern radio jet of B20902 + 343? The naive conclusion from this observed morphology is that the expanding radio source has evacuated its local environs. Such hydrodynamic modification of hot, high filling X-ray emitting cluster gas by expanding radio lobes has been seen in two nearby cluster-center radio sources (Carilli et al. 1994; Bohringer et al. 1993). However it is not clear that such a model can be applied in the case of the dense, low filling factor optical line emitting clouds, and certainly not in the case of the stellar component (assuming that the blue light is stellar in origin). Overall, the spatial coincidence between the 'trough' in the optical images and the northern radio jet of 0902 remains a puzzle.

Acknowledgements. CLC would like to thank T. Muxlow for processing the MERLIN data, M. Dickinson for providing digital versions of the optical images, J.P. Leahy, G. Miley, and C. Lawrence for useful discussions on this topic, N. Jackson and M. Bremer for comments on an early version of this paper, the Director of NRAL for providing discretionary observing time with MERLIN, and the referee, M. Dickinson, for making suggestions which improved this paper. The VLA is a facility of the National Radio Astronomy Observatory, which is operated by Associated Universities Inc. under cooperative agreement with the National Science Foundation.

#### References

Antonucci R.A., 1993, ARAA 31, 473
Barthel P.D., 1989, ApJ 336, 606
Begelman M.C., Blandford R.D., Rees M.J., 1984, Rev. Mod Phys. 56, 255
Briggs F.H., Sorar E., Taramopoulos A., 1993, ApJ 415, L99

Baum S.A., Heckman T., 1989, ApJ 336, 681

Bohringer H., Voges W., Fabian A.C., Edge A., Neumann D., 1993, MNRAS 264, L25

Carilli C.L., Perley R.A., Dreher J.W., and Leahy J.P., 1991, ApJ 383, 554

Carilli C.L., Perley R.A., Dreher J.W., 1988, ApJ 334, L73

Carilli C.L., Owen F., Harris D.E., 1994, AJ. 107, 480

Carilli C.L., Perley R.A., Harris D.E., 1994, MNRAS 270, 173

Chambers K.C., Miley G.K., van Breugel, W., 1987, Nat 329, 604

Dunlop J.S., Hughes D.H., Rawlings S., Eales S.A., Ward M.J., 1994, Nat 370, 347

Dreher J.W., Carilli C.L., Perley R.A., 1987, ApJ 316, 611

Eales S.A., Rawlings S., Puxely P., Rocca-Volmerange B., Kuntz K., 1993, Nat 363, 140

Eales S.A., Rawlings S., 1993, ApJ in press

Eales S.A., Rawlings S., 1990, MNRAS 243, L1p

Eisenhardt P., Dickinson M., 1992, ApJ 399, L47

Harris D.E., Carilli C.L., Perley R.A., 1993, Nat 367, 713

Kapahi V., Murphy D., 1990, in: (eds.) Zensus A., Pearson T., Parsec Scale Radio Jets, Cambridge University Press, Cambridge, p. 313

Leahy J.P., 1987, MNRAS 226, 433

Lilly S.J., 1988, ApJ 33, 161

McCarthy P.J., van Breugel W., Spinrad H., Djorgovski S., 1987, ApJ 321, L29

McCarthy P.J., 1993, ARA&A 31, 639

Meisenheimer K., Roser H.-J., Hiltner P., et al., 1989, A&A 219, 63

Miley G., 1980, ARA&A 18, 165

Muxlow T.W.B., Pelletier G., Roland J., 1988, A&A 206, 237

Pedelty J.A., Rudnick L., McCarthy P.J., Spinrad H., 1989, AJ 97, 647 Perley R.A., 1993, VLA Observing Status Summary, NRAO, Socorro,

NM

Rottgering H., 1993, Ph.D. Thesis, University of Leiden

Stone R.C., 1994, AJ 108, 303

Taylor G., Barton E., Ge G.P., 1994 AJ 107, 1942

Tribble P., 1993, MNRAS 261, 57

Uson J.M., Bagri D.S., Cornwell T.J., 1991, Phys. Rev Lett. 67, 3328 van Breugel W., McCarthy P.J., 1989, in: (eds.) Meurs E.J., Fosbury R.A., Extranuclear Activity in Galaxies, ESO, Munich, p. 227 van Breugel W., Heckman T., Miley G. 1984, ApJ 276, 79